Acta Cryst. (1982). A**38**, 62–67

X-ray Dichroism and Polarized Anomalous Scattering of the Uranyl Ion

BY DAVID H. TEMPLETON AND LIESELOTTE K. TEMPLETON

Materials and Molecular Research Division, Lawrence Berkeley Laboratory and Department of Chemistry, University of California, Berkeley, California 94720, *USA*

(*Received* 2 *April* 1981; *accepted* 15 *June* 1981)

Abstract

Dichroism is observed near the L_1 and L_3 edges of uranium in X-ray absorption spectra of single-crystal rubidium uranyl nitrate, $Rb.UO_2.3NO_3$, recorded with linearly polarized synchrotron radiation. The anomalous X-ray scattering terms f' and f'' calculated from these spectra are anisotropic functions of polarization direction at these wavelengths, adding new complexity to diffraction optics. These terms are measured independently in diffraction experiments with sodium uranyl acetate at five wavelengths near L_3. The cubic symmetry permits the diffraction effects to be observed without the complications of macroscopic dichroism and birefringence. Both f' and f'' change with polarization direction by as much as 2 electrons atom^{-1}. These values agree with those derived from the absorption experiments.

Introduction

In this paper we report observations of X-ray dichroism near the L_1 and L_3 uranium absorption edges in polarized absorption spectra of a crystal of rubidium uranyl nitrate. From these spectra we derive values for the corresponding anomalous scattering terms for uranium as a function of polarization direction and wavelength. This anisotropic anomalous scattering is observed more directly in a diffraction experiment with sodium uranyl acetate, a cubic crystal which cannot exhibit dichroism on a macroscopic scale. The latter experiment demonstrates that the optical consequences of molecular dichroism still operate at the microscopic scale at which the diffraction phenomenon occurs.

After our observation of X-ray dichroism in the vanadyl ion (Templeton & Templeton, 1980, hereafter TT, 1980) with polarized synchrotron radiation at the Stanford Synchrotron Radiation Laboratory (SSRL), the uranyl ion was obvious as another candidate to exhibit this effect with the added feature that its L absorption edges offer two independent sets of electronic transitions. Absorption at the L_1 edge (0·569 Å) involves the $2s$ electrons while that at L_2 and L_3 (0·592 and 0·722 Å) involves $2p$ electrons. Our experiments with uranium were delayed until we gained access to an unfocused beam line because these short wavelengths are not reflected by the focusing mirror of the original apparatus.

Dichroism in rubidium uranyl nitrate

Molecular dichroism can be observed most clearly if the specimen contains a single orientation of the molecules. An example is the salt $RbUO_2(NO_3)_3$ in which the linear O—U—O ions lie on the threefold axes of the rhombohedral crystals (Hoard & Stroupe, 1949; Barclay, Sabine & Taylor, 1965). These crystals are strongly dichroic in visible light, being almost colorless for polarization parallel to the molecular axis and showing the yellow-green color characteristic of uranyl salts in perpendicular polarization. This dichroism is a convenient aid in the selection of suitable single crystals. A redetermination of the crystal structure in collaboration with Dr A. Zalkin (to be reported elsewhere) gave $a = 9{\cdot}384$ (2), $c = 18{\cdot}899$ (4) Å, and uranium–oxygen distances 1·746 (4) Å (uranyl ion) and 2·474 (3) Å (nitrate neighbors), or 1·76 and 2·48 Å respectively after correction for thermal motion according to the riding model.

Crystals were grown by slow evaporation of aqueous solutions made from rubidium nitrate, uranyl nitrate, and a little nitric acid. Many of them were elongated in the c direction with $\{11\bar{2}0\}$ as the prominent faces.

X-ray absorption curves were measured at SSRL with an Enraf–Nonius CAD-4 diffraction apparatus (Phillips, Cerino & Hodgson, 1979) and an unfocused beam line, line I-5. The beam was reflected twice by a channel-cut silicon monochromator crystal [cut for reflection on (220)] to select a wavelength interval 1 or 2 eV wide. With an electron energy of 3·0 GeV in the storage ring, there was a significant intensity of $\lambda/2$ radiation present, but the gate on the scintillation counter rejected most of it. This beam has strong linear polarization with electric vector horizontal.

This procedure was similar to that described for a vanadyl chelate (TT, 1980). Diffraction experiments established the orientation of the crystal. Then each absorption curve was measured at a sequence of

0567-7394/82/010062-06$01.00

wavelengths using an ion chamber in front of the diffractometer and the scintillation counter (at zero angle with beam stop removed) as detectors. The crystal was set with the *c* axis perpendicular to the beam and respectively vertical or horizontal for the perpendicular and parallel spectra. In each case the radiation was incident approximately perpendicular to (110), the largest face of the crystal.

The spectra exhibit substantial dichroism both at the L_1 edge (Fig. 1) and the L_3 edge (Fig. 2), but the details are quite different. The L_2-edge spectra, which we have not yet recorded, are expected to resemble the L_3 spectra on a smaller scale. The structure near the edge (the Kossel structure) involves transitions of inner electrons to unoccupied molecular orbitals. According to selection rules for dipole transitions, these final states have symmetries which are mutually exclusive for excitation of a $2s$ electron at the L_1 edge or a $2p$ electron at L_3. Thus one is not surprised to find differences. At L_3 the energy of the edge inflection is about 1·5 eV higher, and the first maximum 2·5 eV higher in the parallel spectrum than in the perpendicular one. At L_1 the order is reversed and the energy differences much larger: about 12 eV between edge inflections and 17 eV between first maxima. In both cases the spectral features are smeared by the natural widths of the core vacancy levels, 7·43 eV for L_3 and 14·0 eV for L_1 (Krause & Oliver, 1979).

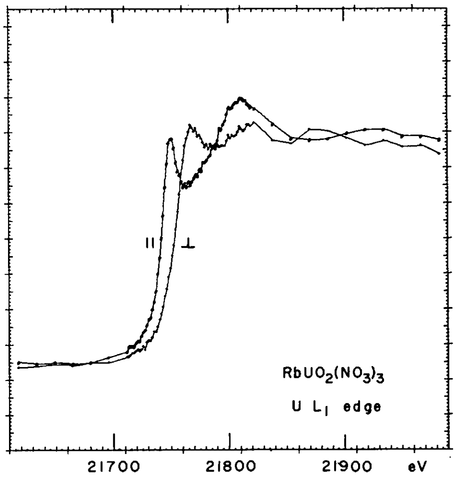

Fig. 1. Absorption coefficient (on an arbitrary scale) *versus* photon energy for polarized X-rays with electric vector parallel and perpendicular to the uranyl axis, near the uranium L_1 edge.

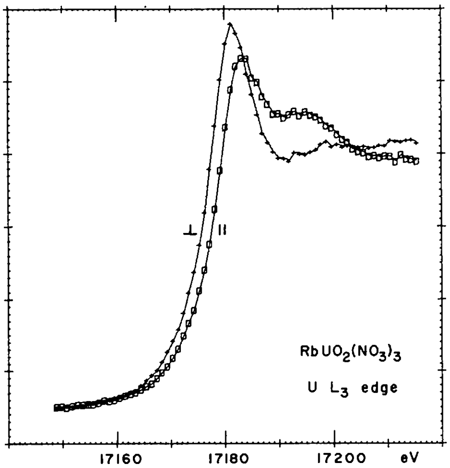

Fig. 2. Same as Fig. 1, but near L_3 edge.

The very complicated electronic structures of the uranyl and other actinyl ions have been studied several times (Yang, Johnson & Horsley, 1978; Denning, Snellgrove & Woodwark, 1979; and references therein), but we fail to find in these works a ready explanation of our results. The final states, in our case, are more like states of neptunyl than uranyl, because an extra electron has been added to the outer shells. The interpretation of these spectra is a challenge which we hope will stimulate further theoretical work.

The dichroism also extends into the EXAFS region, the beginning of which is shown at the right in Fig. 1, and just barely in Fig. 2. Here the absolute magnitude of the effects is smaller, and the consequences to diffraction experiments will be less important. But because they depend on details of the neighboring structure, they will vary from substance to substance. The L_1 spectra can be analyzed like *K*-edge spectra, as in vanadyl acetylacetonate (TT, 1980), with neighbors contributing according to the cosine squared of the angle between each bond and the polarization direction. We do not have independently derived phase shifts for uranium, but with a single phase-shift function we can fit the main features of the parallel curve to the U—O distance 1·76 Å of the uranyl ion and those of the perpendicular curve to the 2·48 Å distance of the nearest nitrate oxygen neighbors. The angular dependence at the L_3 edge is more complicated (Teo & Lee, 1979), with both kinds of neighbors contributing in both polarizations, but again we can fit the largest effects in the two spectra by the two distances. A more detailed discussion is postponed until we have analyzed spectra recorded with better counting statistics than the present ones.

Polarized anomalous scattering

The dielectric constant of a birefringent crystal is given as

$$\varepsilon = \varepsilon_1 c_1^2 + \varepsilon_2 c_2^2 + \varepsilon_3 c_3^2, \qquad (1)$$

where ε_i is the *i*th principal dielectric constant and c_i is a direction cosine of the direction of polarization (electric vector) in the coordinate system of the principal vibration directions (Shubnikov, 1960). In matrix notation, in an arbitrary coordinate system, this becomes

$$\varepsilon = \mathbf{e}^T \boldsymbol{\varepsilon} \mathbf{e}, \tag{2}$$

where $\mathbf{e}$ is a unit column vector describing the polarization, T indicates transpose, and $\boldsymbol{\varepsilon}$ is a tensor. A similar equation describes the absorption cross section of a pleochroic crystal.* The anisotropic dispersion of X-rays follows the same physical principles as visible light, except that one must consider that the wavelength is comparable to interatomic distances. A consequence of this fact is that optical tensors sometimes must be assigned to individual atoms or molecules rather than only to the whole assembly.

Because of the direct relation between X-ray refraction, absorption, and scattering an equation similar to (2) describes the complex anisotropic form factor of an atom which exhibits X-ray dichroism. Consideration of the physics of dipole scattering shows that in this equation the polarization occurs once for the incident ray and again for the scattered ray:

$$f = \mathbf{e}^T \mathbf{f} \mathbf{e}', \tag{3}$$

where $\mathbf{e}'$ is the polarization of the scattered ray and $\mathbf{f}$ is a tensor characteristic of the particular atom at the particular wavelength. The elements of $\mathbf{f}$ are complex numbers. To calculate the total amplitude of scattered radiation one must apply this equation to every combination of each polarization component of the incident ray with each polarization component of the scattering ray, and then combine terms with attention to polarization and phase. The complications become formidable for the general case of a crystal which exhibits significant X-ray dichroism or pleochroism because the double refraction may cause splitting of the rays into components which propagate independently and because different absorption parameters control the attenuation of the various components of both incident and emergent rays.

The situation is more tractable for cubic crystals, very thin crystals, or crystals very dilute in the absorbing atoms. With ordinary light, of course, cubic crystals are optically isotropic. Cubic crystals are also isotropic on a macroscopic scale for propagation or absorption of X-rays. But at the microscopic scale at which diffraction interference occurs, the anisotropy of atoms and molecules affects the intensity of a diffracted ray. The anisotropy considered here is that dependent on polarization of the radiation, and by definition it is treated as a variation of f' and f''; it is quite distinct from the anisotropy of f_0 which reflects any non-spherical electron density and from the anisotropy of thermal motion which is accommodated in the temperature factor.*

We designate by s the polarization direction which is perpendicular to the plane containing the incident and diffracted rays, and by p and p' those which are perpendicular to s (Fig. 3). The symbol f_{sp} means the form factor calculated from (3) with s polarization for the incident ray and p' polarization for the emergent ray, and so on for other combinations. For an isotropic atom with form factor f_n, $\mathbf{f} = [f_n,0,0; 0,f_n,0; 0,0,f_n]$, and

$$f_{ss} = f_n \tag{4a}$$

$$f_{pp} = f_n \cos 2\theta \tag{4b}$$

$$f_{sp} = f_{ps} = 0. \tag{4c}$$

When all the atoms in the crystal are isotropic and the radiation is not polarized, the total amplitudes for the emergent s and p' rays differ just by the factor $\cos 2\theta$ of (4b); addition of the squares then gives a total intensity proportional to $(1 + \cos^2 2\theta)$, the familiar polarization factor for this case. Thus one sees that the polarization factor is included implicitly in (3).

For an anisotropic atom, even in a cubic crystal, the results are more complicated; in general f_{sp} and f_{ps} are not zero, the ratio of f_{pp} to f_{ss} is not exactly $\cos 2\theta$, and f_{pp} may not vanish at $\theta = 45°$.

In our experimental arrangement with synchrotron radiation the incident radiation is highly polarized in the s direction, and we neglect the f_{pp} and f_{ps} terms. Further, in the uranium experiment the f_{sp} amplitude is at most about 2% of f_{ss} and therefore has a negligible effect on the total intensity. In sodium uranyl acetate each uranyl ion lies on a threefold axis, and thus the tensor $\mathbf{f}$ must be uniaxial. We found it convenient to express $\mathbf{f}$ in terms of $f_\sigma = f_0 + f'_\sigma + if''_\sigma$ and $f_\pi = f_0 + f'_\pi$

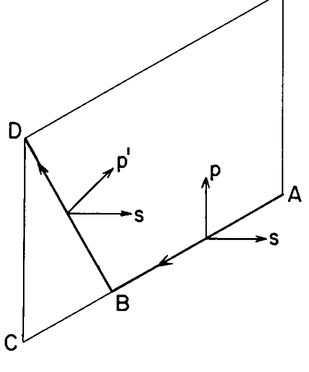

Fig. 3. Definition of polarization directions. The crystal is at B. The incident ray AB, the diffracted ray BD, and polarization directions p and p' all lie in the plane $ABCDE$. Polarization direction s is perpendicular to this plane.

---

* *Pleochroism* is absorption which is different in three principal directions. *Dichroism* is sometimes used in this more general sense, and sometimes restricted to cases where uniaxial symmetry is present, as in the uranyl salts considered here.

* We neglected complications due to optical activity, which in principle may rotate the plane of polarization, but which is expected to be unimportant in the present experiments.

$+ if_\pi''$, the principal values parallel and perpendicular to the symmetry axis respectively. Then $\mathbf{f} = [f_\pi,0,0; 0,f_\pi,0; 0,0,f_\sigma]$ if z is the molecular axis. Because the anisotropy is the quantity we are most interested in here, and the spherical average [equal to $(f_\sigma + 2f_\pi)/3$] is the quantity to compare with ordinary isotropic values, we chose as independent parameters for least-squares adjustment the following:

$$f' = (f_\sigma' + 2f_\pi')/3 \tag{5a}$$

$$f'' = (f_\sigma'' + 2f_\pi'')/3 \tag{5b}$$

$$f_2' = f_\sigma' - f_\pi' \tag{5c}$$

$$f_2'' = f_\sigma'' - f_\pi''. \tag{5d}$$

Then, neglecting all terms except f_{ss}, f can be expressed as

$$f = f_0 + f' + if'' + (\cos^2\alpha - \tfrac{1}{3})(f_2' + if_2''), \tag{6}$$

where α is the angle between the electric vector and the molecular axis. The reader is reminded that f is different for atoms in different molecular orientations, just as the anisotropic thermal tensor is different. But whereas the temperature factor of an atom is the same for a particular *hkl*, whatever the azimuthal orientation of the diffraction experiment, in general the anisotropic f changes for an azimuthal rotation. Thus it is not enough to record intensities as a function of *hkl*; one needs also a record of the orientation of the crystal with respect to the polarization direction.

Modification of our least-squares program (Templeton & Templeton, 1978; hereafter TT, 1978) to determine the new variables was straightforward, once the angles α were calculated. The derivatives with respect to f' and f'' are unchanged, while

$$\frac{\partial|F|}{\partial f_2'} = [\cos^2\alpha - \tfrac{1}{3}]\,\frac{\partial|F|}{\partial f'} \tag{7}$$

and similarly for f_2''.

Sodium uranyl acetate diffraction experiment

Sodium uranyl acetate is cubic, space group $P2_13$, with uranyl ions situated on threefold axes which point in four different directions. The structure was determined, except for hydrogen atoms, by Zachariasen & Plettinger (1959), after an earlier study by Fankuchen (1935). For our experiments we desired a more precise description. A redetermination in collaboration with A. Zalkin and H. W. Ruben (to be reported elsewhere) included hydrogen atoms and, for all heavier atoms, anisotropic thermal parameters. For 1195 independent reflections measured with Mo $K\alpha$ radiation, $R = 0{\cdot}021$. The parameters from this refinement were used without adjustment in the calculation of scattering factors from the synchrotron radiation data.

Crystals of sodium uranyl acetate were grown by slow evaporation of solutions containing excess acetic acid. Some of them were twinned. We used one with dimensions about 0·14 × 0·20 × 0·30 mm, bounded by 13 faces including $(\bar{1}\bar{1}1)$ and all of $\{110\}$. Its enantiomeric purity was verified (within a few percent) by comparison of calculated Bijvoet ratios with several measured with Mo $K\alpha$ radiation.

The technique of the diffraction experiment was similar to that described by Templeton, Templeton, Phillips & Hodgson (1980). The data at 0·72157 Å were measured at SSRL beam line I-5 with the channel-cut silicon 220 monochromator. The rest of the work was done at beam line II-2, with the focusing mirror dropped out of the optical path. The monochromator consisted of two independent silicon 220 crystals, which were slightly misaligned to reduce the intensity of higher-order reflections. Removing the mirror is necessary because the critical angle for reflection of 0·7 Å radiation is too small for the mirror design. It has the additional benefit that the radiation is more nearly monochromatic, with energy spread of the order of 1 eV (0·00004 Å), than if a mirror were used; focusing introduces convergence in the beam directions and thus a range of monochromator angles. Checks of the wavelength by measurement of absorption curves indicate that it changed about 0·00006 Å (or 1·5 eV) during the 12 h of the experiment at 0·72147 Å, but changed no more than half as much in any of the other runs.

Diffraction data for the line I-5 experiment were collected in the 'zigzag' mode for reflections in the range θ = 3 to 25°, each at ψ = 0°. The other sets included reflections with θ = 3 to 20°, each measured at three azimuthal settings, ψ = −30, 0, and 30°. No set was complete, and the number of data (Table 1) was influenced by the available time and problems with the equipment. Many of these data would be duplications according to cubic symmetry. The polarization effects break the symmetry, and each reflection, even at each different azimuthal angle, must be treated as an

Table 1. *Anisotropic anomalous scattering terms from diffraction experiment with sodium uranyl acetate*

λ (Å)	0·72177	0·72170	0·72157	0·72147	0·72124
f'	−19·4 (3)	−19·1 (3)	−16·0 (4)	−14·3 (4)	−13·4 (3)
f_2'	−0·2 (3)	−0·1 (3)	−1·7 (4)	−1·8 (4)	−0·7 (3)
f_σ'	−19·5 (4)	−19·2 (4)	−17·1 (5)	−15·5 (5)	−13·9 (4)
f_π'	−19·3 (3)	−19·1 (3)	−15·4 (4)	−13·7 (4)	−13·2 (3)
f''	10·2 (4)	13·1 (3)	16·1 (5)	13·2 (6)	12·2 (5)
f_2''	−1·7 (3)	−2·1 (3)	−1·1 (3)	0·1 (4)	1·7 (3)
f_σ''	9·1 (4)	11·7 (4)	15·4 (5)	13·3 (7)	13·3 (5)
f_π''	10·8 (4)	13·8 (3)	16·5 (5)	13·2 (6)	11·6 (5)
R (%)	3·4	3·8	3·8	4·4	3·8
n*	723	1125	643	869	759

* Number of reflections.

independent measurement with its own calculated structure factor.

Intensities were normalized according to readings of an ion chamber in front of the entrance collimator, to correct for changes of beam intensity. Within each data set the correction factors varied by a factor of two or less. This work was done at times of 'dedicated' operation (no positrons in the storage ring), mostly with the beam relatively free of short-term variations and with long-term decay with half-life of many hours. Because a movement of the beam position affects the intensity at the crystal more than at the larger ion chamber, this method of monitoring was imperfect. Intensities of a frequently measured standard reflection, after correction according to the ion chamber, varied with standard deviations of 4 to 7% in the various data sets. This variation is enough to explain most of the discrepancy indicated by the *R* factors listed in Table 1.

Intensities were corrected for absorption with our analytical absorption program. Correction factors ranged from about 3·7 to 10·0. They were corrected by the Lorentz factor but not for polarization.

The results derived by least-squares adjustment are listed in Table 1. The anisotropy parameters f_2' and f_2'' are plotted in Fig. 4, where the points with error bars are the results of this diffraction experiment. The curves were derived from the absorption curves for the rubidium salt using equations given by TT (1980). The curve for $f_\sigma'' - f_\pi''$ is essentially the difference of the two curves in Fig. 2, scaled to correspond to known values of f''. The curve for $f_\sigma' - f_\pi'$ was derived by integrating the Kramers–Kronig dispersion relation over the narrow interval where dichroism is significant. The agreement between the results of the two methods is gratifying.

The parallel and perpendicular values of f' and f'' are plotted against wavelength in Fig. 5. These principal values are extremes; values for an intermediate angle will fall between the pairs of curves.

These effects are enhanced by the polarized nature of synchrotron radiation, but they will occur even with unpolarized incident radiation; the scattering process always introduces some polarization into the scattered ray.

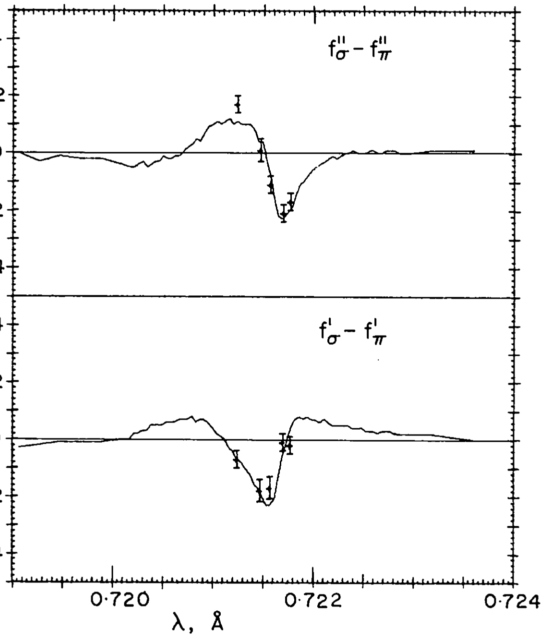

Fig. 4. Polarization anisotropy of f' and f'' for the uranyl ion near the L_3 edge, measured in the diffraction experiments (points with error bars) and the absorption experiment (continuous curves).

Conclusion

Until now anomalous X-ray scattering has been treated in diffraction experiments as an isotropic effect which is independent of molecular orientation. We pointed out earlier (TT, 1980) that this does not hold when dichroism occurs. The present work demonstrates for the first time that the effects can be observed in diffraction intensities, and that they agree in magnitude with those derived from absorption measurements. This effect adds a new dimension of complexity to the theory of X-ray scattering. By introducing an error into the

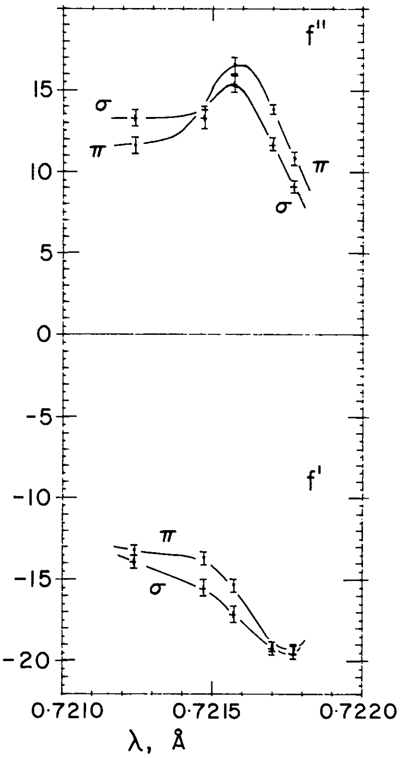

Fig. 5. Principal values of the anisotropic f' and f'' for the uranyl ion, measured in the diffraction experiment.

conventional methods of computation, it offers a handicap to the use of anisotropic molecules like the uranyl ion to exploit the maximum effects at the absorption edges for solving the phase problem. Thus from a pessimistic point of view it is a setback. We adopt the opposite view: where there is a complication there is the opportunity of sharper, more penetrating methods for extracting information from diffraction experiments. There is much to look for in the exploration of this new region of diffraction optics.

Mrs Helena W. Ruben grew some of the crystals we used. We thank her and Dr Allan Zalkin for cooperation in the structure determinations needed for this work and Dr Paul R. Phizackerley and Professor Keith O. Hodgson for assistance with the apparatus at SSRL. This work was supported by the National Science Foundation under Grant No. CHE-7919532. It used facilities of SSRL with support of the NSF under Contract DMR77-27489 (in cooperation with the Department of Energy) and the Lawrence Berkeley Laboratory, supported by the Director, Office of Energy Research, Office of Basic Energy Sciences, Chemical Sciences Division of the US Department of Energy under Contract No. W-7405-Eng-48.

References

Barclay, G. A., Sabine, T. M. & Taylor, J. C. (1965). *Acta Cryst.* **19**, 205–209.

Denning, R. G., Snellgrove, T. R. & Woodwark, D. R. (1979). *Mol. Phys.* **37**, 1109–1143.

Fankuchen, I. (1935). *Z. Kristallogr.* **91**, 473–479.

Hoard, J. & Stroupe, J. (1949). *Nat. Nucl. En. Series Div.* 3, Vol. 2, ch. 2, pp. 15–35.

Krause, M. O. & Oliver, J. H. (1979). *J. Phys. Chem. Ref. Data*, **8**, 329–338.

Phillips, J. C., Cerino, J. A. & Hodgson, K. O. (1979). *J. Appl. Cryst.* **12**, 592–600.

Shubnikov, A. V. (1960). *Principles of Optical Crystallography*, pp. 48, 181. New York: Consultants Bureau.

Templeton, D. H. & Templeton, L. K. (1980). *Acta Cryst.* A**36**, 237–241.

Templeton, D. H., Templeton, L. K., Phillips, J. C. & Hodgson, K. O. (1980). *Acta Cryst.* A**36**, 436–442.

Templeton, L. K. & Templeton, D. H. (1978). *Acta Cryst.* A**34**, 368–371.

Teo, B.-K. & Lee, P. A. (1979). *J. Am. Chem. Soc.* **101**, 2815–2832.

Yang, C. Y., Johnson, K. H. & Horsley, J. A. (1978). *J. Chem. Phys.* **68**, 1001–1005.

Zachariasen, W. H. & Plettinger, H. A. (1959). *Acta Cryst.* **12**, 526–530.

Acta Cryst. (1982). A**38**, 67–70

The Influence of the Elimination of Low-Intensity Data on the Applicability Range of R_2 in Automated Structure Evaluations

By G. H. Petit and A. T. H. Lenstra

University of Antwerp (UIA), Department of Chemistry, Universiteitsplein 1, B-2610 Wilrijk, Belgium

(*Received* 27 *April* 1981; *accepted* 4 *June* 1981)

Abstract

A description is given of the effect on the residual R_2 caused by a misplacement of a fraction of the atoms in a tentative structure model. New expressions are derived for the space groups $P1$ and $P\bar{1}$ for moments as functions of the threshold a, below which intensity data are omitted. It turns out that the range in which R_2 acts as a discriminator between correct and incorrect models is drastically limited even by low threshold values. Theory and experiment are shown to be in excellent agreement.

Introduction

Automation of a crystal structure analysis requires criteria which discriminate between a correct and an incorrect set of atomic positions. If one decides to use mathematical functions for this purpose, then residual functions are an obvious choice (Lenstra, 1974). In this article we will discuss some properties of R_2, which is defined as

$$R_2 \equiv \frac{\sum_H (E_N^2 - E_n^2\,\sigma_1^2)^2}{\sum_H E_N^4}, \qquad (1)$$

where E_N^2 corresponds to the observed normalized intensities and E_n^2 to the normalized intensities related to the tentative fragment of the structure; σ_1^2 is given by $\sum_{j=1}^{n} f_j^2/\sum_{j=1}^{N} f_j^2$.

Let the structure looked for contain N equal atoms and let the tentative structure model contain n atoms ($n \le N$), of which g atoms are correctly located and f atoms are badly misplaced ($g + f = n$). This model is